Surface Redox Pseudocapacitance of Partially Oxidized Titanium Carbide MXene in Water-in-Salt Electrolyte

Wang, Xuehang; Bak, Seong Min; Han, Meikang; Shuck, Christopher E.; Mchugh, Conlan; Li, Ke; Li, Jianmin; Tang, Jun; Gogotsi, Yury

DOI
10.1021/acsenergylett.1c02262

Publication date
2022

Document Version
Final published version

Published in
ACS Energy Letters

ACS Energy LETTERS

http://pubs.acs.org/journal/aelccp

Surface Redox Pseudocapacitance of Partially Oxidized Titanium Carbide MXene in Water-in-Salt Electrolyte

Xuehang Wang,[‖] Seong-Min Bak,[‖] Meikang Han, Christopher E. Shuck, Conlan McHugh, Ke Li, Jianmin Li, Jun Tang, and Yury Gogotsi*

Cite This: *ACS Energy Lett.* 2022, 7, 30−35

Read Online

ACCESS | Metrics & More | Article Recommendations | Supporting Information

ABSTRACT: **Achieving pseudocapacitive intercalation in MXenes with neutral aqueous electrolytes and driving reversible redox reactions is scientifically appealing and practically useful. Here, we report that the partial oxidation of MXene intensifies pseudocapacitive Li^+ intercalation into $Ti_3C_2T_x$ MXene from neutral water-in-salt electrolytes. An *in situ* X-ray absorption near-edge structure analysis shows that the Ti oxidation state changes during the Li^+ intercalation, indicating the presence of a surface redox reaction. The Ti oxidation/reduction is further confirmed by an *in situ* extended X-ray absorption fine structure analysis, which shows a reversible contraction/expansion of the Ti−C interatomic distance. The intensified Li^+ pseudocapacitive intercalation can be explained by the higher oxidation state of Ti at the open circuit potential. This work demonstrates the possibility of tuning the pseudocapacitive intercalation by adjusting the initial oxidation state of the transition metal on the MXene and offers a facile way to enhance the pseudocapacitance of various MXenes.**

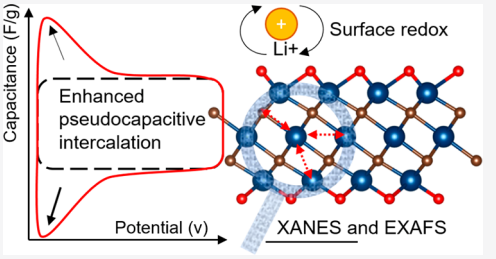

The rapidly growing demand for electrochemical energy storage motivates the development of devices that combine high energy density and power density, while being safe to use.[1] The use of pseudocapacitive electrode materials, which can store more charge in comparison to electrical double-layer capacitors and allows for faster charging rates than batteries, is attractive but requires a proper coupling of active materials and electrolytes.[2] MXenes, a large family of two-dimensional (2D) transition-metal carbides and/or nitrides, are promising high-rate pseudocapacitive materials due to their metallic conductivity, ionic channels between 2D sheets, and redox-active surface.[3] The general formula of MXene is $M_{n+1}X_nT_x$ (n = 1−4), where M is a transition metal(s), X is carbon/nitrogen, and T_x is the surface functional groups (typically =O, −OH, −Cl, and −F).[4,5] In acidic aqueous electrolytes, titanium carbide ($Ti_3C_2T_x$), the most widely used MXene, is capable of delivering high volumetric capacitance along with an excellent rate capability.[6] The charge storage of $Ti_3C_2T_x$ in acidic aqueous electrolytes is attributed to the fast pseudocapacitive proton intercalation/deintercalation with a surface redox reaction (protonation of the oxygen-terminated surface). The surface redox reaction between the intercalated proton and the MXene surface groups involves a partial electron transfer with corresponding modification of the Ti atom oxidation state of the $Ti_3C_2T_x$ surface layers.[7,8]

In comparison with acidic aqueous electrolytes, titanium carbides show weak pseudocapacitive ion intercalation in less-corrosive neutral electrolytes.[9] Only a minor valence change of Ti was observed during Li^+ intercalation in Ti_2CT_x with an operating window of −0.2 to −0.7 V vs Ag/Ag^+.[10] The surface redox between Li^+ and the MXene surface is stronger at more negative potentials, and peaks can be observed in CV curves.[11] For example, an intensified pseudocapacitive intercalation of Li^+ was observed for $Ti_3C_2T_x$ at a negative potential below −1.2 V vs Ag wire in Li^+-based organic electrolytes.[12] Strong Li^+ pseudocapacitive intercalation was also observed below 2 V vs Li/Li^+ in an Li^+-based organic electrolyte for $Ti_3C_2Cl_2$.[13] Using water-based electrolytes is safer than using organic electrolytes and avoids the formation of a solid−electrolyte interphase. However, due to the easy water electrolysis and hydrogen evolution on MXenes, enhanced Li^+ pseudocapacitance with surface redox is not observed within the applicable potential window of MXenes in neutral aqueous electrolytes.

Received: October 16, 2021
Accepted: November 22, 2021
Published: November 24, 2021

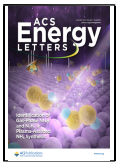

https://doi.org/10.1021/acsenergylett.1c02262
ACS Energy Lett. 2022, 7, 30−35

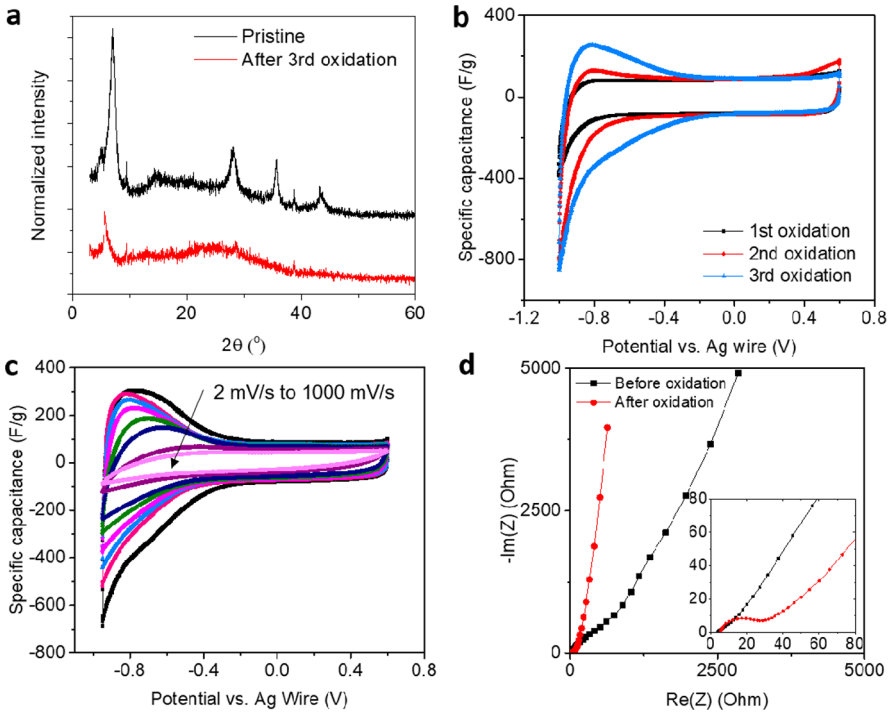

Figure 1. (a) X-ray diffraction pattern of $Ti_3C_2T_x$ before and after *in situ* oxidation. (b) Cyclic voltammograms (CVs) of $Ti_3C_2T_x$ electrodes *in situ* oxidized at 1.2 V vs Ag wire in 19.2 m LiBr. The CVs were collected at a scan rate of 2 mV/s, which is the same as the oxidation process. (c) CVs of the partially oxidized $Ti_3C_2T_x$ at scan rates of 2, 10, 20, 50, 100, 200, 500, and 1000 mV/s. (d) Nyquist plots before and after *in situ* oxidation of $Ti_3C_2T_x$ in 19.2 m LiBr. The inset shows a magnified view of the impedance spectra in the high-frequency range.

Using water-in-salt (WIS) electrolytes has been reported to enlarge the negative potential window of titanium carbide MXene electrodes,[14−16] but still, no redox accompanying Li^+ intercalation has been observed.

This work reports on the enhanced Li^+ pseudocapacitive intercalation at a negative potential on partially oxidized $Ti_3C_2T_x$ in WIS electrolytes. The activated Li^+ surface redox below −0.2 V vs Ag improves the $Ti_3C_2T_x$ charge storage capacity in neutral aqueous electrolytes. On the basis of *in situ* X-ray absorption spectroscopy (XAS), the Ti valence reversibly changes between +2.78 and +2.86 during the charge/discharge process on the partially oxidized $Ti_3C_2T_x$ electrode. The Ti valence of partially oxidized $Ti_3C_2T_x$ at the open circuit potential is higher than the nonoxidized species, explaining the stronger Li^+ pseudocapacitive intercalation between MXene sheets within the potential window in the WIS electrolytes. This finding demonstrates that the initial oxidation state of the transition metal is crucial for the ion pseudocapacitive intercalation processes in MXenes.

Pristine $Ti_3C_2T_x$ was oxidized *in situ* in a 19.2 m (mol/kg of solvent) LiBr WIS electrolyte by cyclic voltammetry between 0 and 1.2 V vs Ag at a scan rate of 2 mV/s (Figure S1a). Notably, $Ti_3C_2T_x$ is electrochemically stable up to 0.8 V vs Ag in 19.2 m LiBr.[17] X-ray diffraction (XRD) shows the (002) peak of $Ti_3C_2T_x$ before and after three oxidation cycles (Figure 1a). This suggests that $Ti_3C_2T_x$ was not completely oxidized into TiO_2 after the *in situ* oxidation at an applied potential of 1.2 V. The high stability of $Ti_3C_2T_x$ could be attributed to the lower activity of water in the WIS electrolyte.[18] The (002) peak shifts from 7° to 5.6° after *in situ* oxidation, meaning that the $Ti_3C_2T_x$ *d* spacing increased from 12.6 to 15.7 Å. The enlarged interlayer space after partial oxidation was also observed for $Ti_3C_2T_x$ in the H_2SO_4 electrolyte.[19] A broad XRD peak (20−40°) is observed in the *in situ* oxidized sample, corresponding to the trace level of amorphous titania or carbon formation.[20] Because the oxidation of the MXene is regulated at a low level in this study (Figure S1), the formation and contribution of these minor impurity phases to the total capacitance are expected to be minimal.

Prior to oxidation, $Ti_3C_2T_x$ showed a rectangular cyclic voltammogram (CV) curve in the potential window of −1.1 to +0.5 V vs Ag in a 19.2 m LiBr electrolyte. After the first oxidation cycle, the CV curve is almost mirrorlike, with a pair of peaks emerging from about −0.4 V to the most negative potential (Figure 1b). The intensity of the peaks increases after each oxidation cycle and becomes significant after three *in situ* oxidation cycles. The peaks that emerged at the negative potential window in the CVs correspond to a reversible process, since the Coulombic efficiency is above 95%. Chronoamperometry tests show a steady-state leakage current of <0.1 A/g until −1.0 V vs Ag in 19.2 m LiBr electrolyte (Figure S2). The small leakage current excludes the possibility of hydrogen storage or evolution under the applied potential. Furthermore, the high capacitance retention of the partially oxidized MXene (105% after 10000 cycles at 100 mV/s) suggests excellent cycling stability within the 1.6 V potential range from −1.1 to +0.5 V vs Ag (Figure S6). Similarly, the $Ti_3C_2T_x$ electrode after the *in situ* oxidization in 19.8 m LiCl electrolyte also shows a strong pair of peaks between −0.2 and −1.1 V vs Ag on the cathodic and anodic branches of the CV curves (Figure S3). The capacitance of $Ti_3C_2T_x$ after oxidation at 2 mV/s increases about 54% to 154 F/g (385 F/cm^3) in 19.2 m LiBr and 55% to 116 F/g (290 F/cm^3) in 19.8 m LiCl.

The peaks in CVs are located at similar potentials on the cathodic and anodic branches, suggesting pseudocapacitive intercalation.[21] Calculating the *b* value can give an indication

https://doi.org/10.1021/acsenergylett.1c02262
ACS Energy Lett. 2022, 7, 30−35

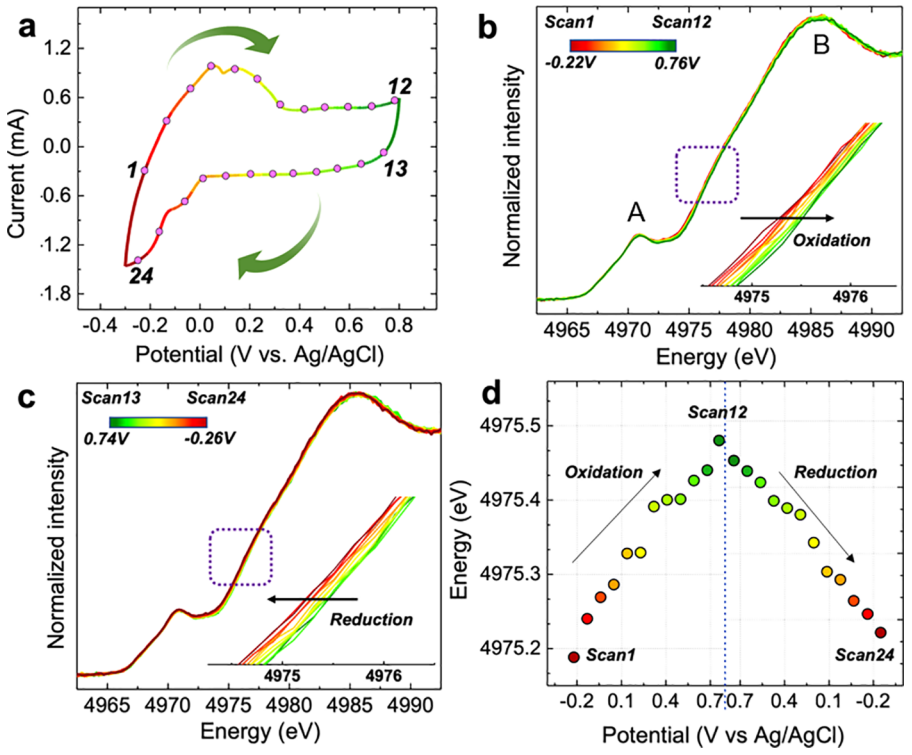

Figure 2. (a) Cyclic voltammogram collected in an *in situ* time-resolved X-ray absorption spectroscopy (XAS) electrochemical cell at 2 mV/s in 19.2 m LiBr aqueous electrolyte. The points on the CV curves represent the charging stage when the XAS scan is performed. Corresponding Ti K-edge X-ray absorption near edge structure (XANES) spectra of partially oxidized $Ti_3C_2T_x$ during (b) anodic scans, (c) cathodic CV scans, and (d) variation of Ti K-edge energy (at half-height of normalized XANES spectra).

of the dominating charge storage mechanism of the process.[22] The *b* value was obtained by plotting the logarithm of the peak current (log i_p) on the discharge branch of the CV curves as a function of the logarithm of the scan rate (log v) and estimating the slope of the curve (log i_p = log a + b log v). The slopes of the log i_p–log v curve are close to 1 for the partially oxidized MXene in both LiCl and LiBr electrolytes (Figure S4). This means that the electrochemical processes corresponding to the peaks in CVs are surface-controlled. The oxidized $Ti_3C_2T_x$ electrodes with surface-controlled charging processes show good rate performance in both LiBr (Figure 1c) and LiCl electrolytes (Figure S5a). The partially oxidized $Ti_3C_2T_x$ delivers capacitances of 85 F/g at 100 mV/s and 40 F/g at 1,000 mV/s in the highly concentrated LiBr electrolyte (Figure S5b).

Electrochemical impedance spectroscopy was performed on the $Ti_3C_2T_x$ electrode before and after oxidation in both 19.2 m LiBr (Figure 1d) and 19.8 m LiCl (Figure S2b). The slopes of the Nyquist plot at low frequencies are closer to 90° for the oxidized $Ti_3C_2T_x$ electrodes in both electrolytes, indicating that the charge storage processes are less diffusion limited after oxidation. The width of the Warburg region at midfrequencies of impedance, which reflects the length of ion diffusion, is also shorter for the oxidized samples. The equivalent series resistance (ESR) of the partially oxidized $Ti_3C_2T_x$ is similar to the pristine species, indicating that the electrode conductivity is not significantly affected. Magnified impedance spectra at high frequencies show that a small semicircle emerges after the partial oxidation in both electrolytes. The emerging semicircle suggests the presence of charge transfer in the partially oxidized samples, which agrees with the intensified pseudocapacitive intercalation observed in CVs.

In order to understand the charge storage process in the partially oxidized $Ti_3C_2T_x$, we performed *in situ* time-resolved X-ray absorption spectroscopy (TR-XAS). Synchrotron-based XAS techniques have been successfully used to provide direct evidence for the pseudocapacitance of MXenes by tracking changes in the metal edge position during electrochemical cycling in both aqueous and nonaqueous electrolyte systems.[7,23] Herein, *in situ* X-ray absorption near-edge structure (XANES) and extended X-ray absorption fine structure (EXAFS) were used to provide direct evidence of charge transfer (redox) and local structural changes, respectively, upon Li^+ intercalation/deintercalation of the partially oxidized $Ti_3C_2T_x$ during CV scans. To obtain a good signal to noise ratio for the Ti K-edge XAS spectra and reliable electrochemical performance, a plastic pouch cell with a three-electrode configuration was used (see Figure S7 in the Supporting Information). The CV obtained with the *in situ* electrochemical cells (Figure 2a) successfully reproduced the strong peaks observed in the three-electrode Swagelok cell.

In situ Ti K-edge TR-XAS spectra were collected during cyclic voltammetry in 19.2 m LiBr at 2 mV/s. Thanks to the high radiation brilliance at the QAS beamline at the National Synchrotron Light Source II, satisfactory data quality to study the electrochemical process with sufficient time resolution could be achieved. It is noteworthy that previous *in situ* XAS studies on pseudocapacitive materials utilized a quasi *in situ* approach due to the limit of the XAS signal acquisition time (usually >15 min).[24] For example, the applied potentials during CV were held constant for a while (e.g., ~25 min) until a steady-state current was attained.[7] In this study, the acquisition time for each XAS spectra only took 37 s, enabling

https://doi.org/10.1021/acsenergylett.1c02262
ACS Energy Lett. 2022, 7, 30−35

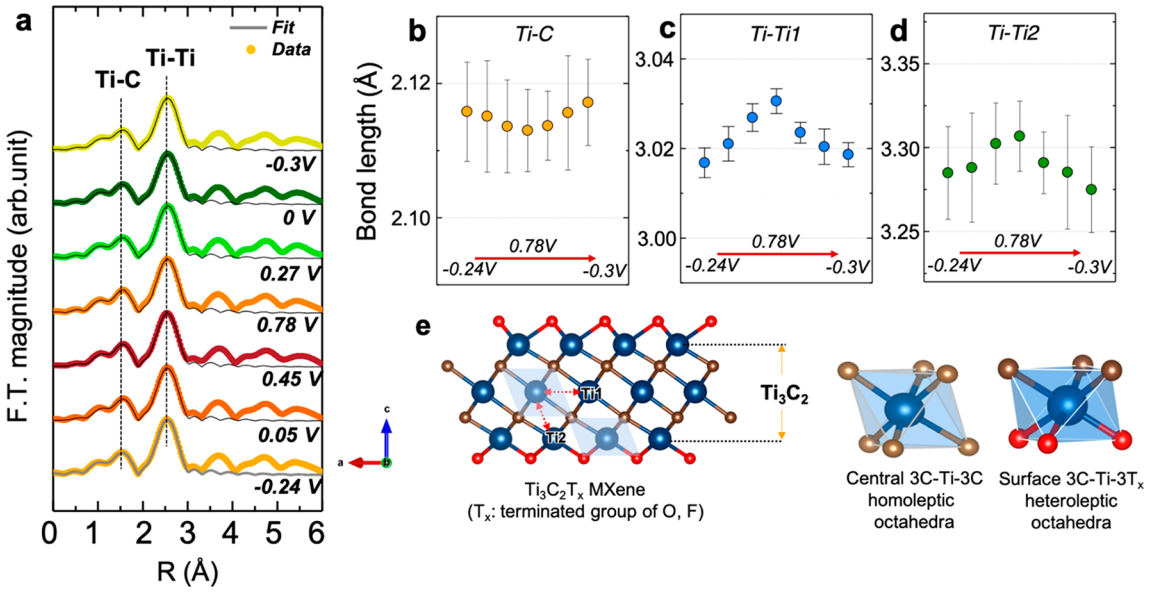

Figure 3. (a) *In situ* extended X-ray absorption fine structure (EXAFS) analysis of partially oxidized $Ti_3C_2T_x$ at different potentials. (b–d) Changes in Ti–C, Ti–Ti1 and Ti–Ti2 bond lengths with potential, respectively. (e) Schematic illustrations of the Ti–C, Ti–Ti1, and Ti–Ti2 bonds in the $Ti_3C_2T_x$ MXene.

us to monitor the electrochemical processes in a continuous manner.

The corresponding Ti K-edge XANES spectra of $Ti_3C_2T_x$ during the anodic and cathodic scans are presented in Figure 2b,c, respectively. All of the Ti K-edge XANES spectra show a relatively weak pre-edge peak (marked as A) at 4971 eV and a strong main absorption peak (marked as B) at around 4985 eV. The pre-edge A peak is associated with the transition from the Ti 1s core state to hybridized electronic states of the metal 3d and carbon 2p orbitals.[7,25] In the case of $Ti_3C_2T_x$, the A peak can be assigned to the transition of a 1s electron to hybridized t_{2g} (Ti 3d + C 2p) and e_g (Ti 3d + C 2p) orbitals. The main absorption B peak is attributed to the dipole-allowed transition of a 1s electron to unoccupied Ti 4d states. The spectra for each scan do not show significant differences in shapes, but the edge shift is observable in both the anodic and cathodic scans (insets in Figure 2b,c). During the anodic potential scan (measured from −0.22 to +0.76 V), the edge shifts to higher energies, reflecting the oxidation of titanium. During the cathodic scan (measured from +0.74 V to −0.26 V), the edge shifts back to lower energies, indicating the reduction of titanium. A plot of the Ti K-edge energies at half-height of normalized XANES spectra, as a function of potential in Figure 2d, clearly shows the consistent energy position changes and their reversibility during the anodic and cathodic scans. The reversible change of the Ti K-edge energy during charge/discharge suggests the presence of surface redox reactions during the Li^+ intercalation and deintercalation.

While XANES probes the electronic structure changes of a selected atom (i.e., the oxidation state of Ti in this study), EXAFS can provide the local structural changes such as bond length changes and ordering/disordering. Figure 3 shows the Fourier-transformed EXAFS collected during the CV scan. The first shell (Ti–C) and second shell (Ti–Ti) EXAFS fitting was performed in an *R* range of 1.2–3.1 Å. The fitted values for interatomic distances of Ti–C, Ti–Ti1, and Ti–Ti2 are plotted in Figure 3b–d, respectively. As described in Figure 3e, two different Ti–Ti bond lengths (central 3C–Ti–3C homoleptic octahedra and surface 3C–Ti–3T_x heteroleptic octahedra) were used in EXAFS fitting. We approximate this model into short Ti–Ti1 and long Ti–Ti2 bond lengths for facile EXAFS fitting, leading to improved fitting parameters. The EXAFS fitting shows a decrease in Ti–C distance and an increase of both Ti–Ti distances during the anodic scan. Meanwhile, the opposite was observed during the cathodic scan: an increase in Ti–C distance and decreases in Ti–Ti distances. These interatomic distance changes are associated with the Li^+ intercalation/deintercalation in $Ti_3C_2T_x$ during the cathodic and anodic CV scans. During the Li^+ intercalation process, the Ti atoms are reduced (as shown by XANES), shortening the Ti–C bond. The opposite behavior was observed during the Li^+ deintercalation process, with the changes being reversible. The reversible contraction/expansion interatomic distance associated with Ti valence state changes confirms the redox-active charge storage mechanisms of $Ti_3C_2T_x$ in the LiBr electrolyte.

For nonoxidized $Ti_3C_2T_x$, the valence of Ti changes between +2.43 and +2.34 in the H_2SO_4 electrolyte, on the basis of our previous study.[7] In this study, the initial valence of Ti in the partially oxidized $Ti_3C_2T_x$ is higher, at about +2.86. The partially oxidized $Ti_3C_2T_x$ shows a distinct normalized Ti K-edge XANES spectrum in comparison to both the TiO and TiO_2 reference spectra (Figure S8a). This indicates that the oxidation of $Ti_3C_2T_x$ into titania (if any) is minor. The partial oxidation of $Ti_3C_2T_x$ is directly proved by the Ti $L_{2,3}$-edge soft XAS, which shows spectral changes reflecting the oxidation state change of Ti (Figure S9). The electrochemical oxidation and reduction process of the partially oxidized $Ti_3C_2T_x$ is reversible—the Ti valence of the partially oxidized $Ti_3C_2T_x$ changes between +2.78 and +2.86 during the cycling process. The higher initial valence of Ti in the partially oxidized $Ti_3C_2T_x$ explains the enhanced pseudocapacitive intercalation at <−0.2 V vs Ag, as Ti (+2.86) is more prone to be reduced than Ti (+2.43).

The surface redox reaction, which involves partial electron transfer, contributes to the overall capacitance of the partially

https://doi.org/10.1021/acsenergylett.1c02262
ACS Energy Lett. 2022, 7, 30–35

oxidized MXene electrode. On the basis of the *in situ* XANES, the average Ti oxidation state change during charge/discharge is ~0.24 e (i.e., an average of 0.08 e per Ti atom) over a potential window of 1.1 V (Figure S8b). When the overall formula weight of $Ti_3C_2O_2$ is assumed to be ~202 g/mol, the value of electron transfer corresponds to a specific capacitance of about 104.2 F/g. On the basis of this semiempirical estimation, the surface redox reaction contributes 67% of the overall capacitance of the partially oxidized $Ti_3C_2T_x$ electrode in the 19.2 m LiBr. Hence, the charge storage of partially oxidized $Ti_3C_2T_x$ is dominated by pseudocapacitance and is based on the redox reactions centered at Ti. The emerging surface redox reaction at a negative potential explains the dramatic capacitance increase after partial oxidation of $Ti_3C_2T_x$ in the neutral WIS electrolytes.

An appreciation of this new pseudocapacitive energy storage mechanism under negative potential in partially oxidized $Ti_3C_2T_x$ allows for the search of other MXenes with even less negative redox potentials and a large overpotential for hydrogen evolution reaction,[26] which may show higher capacitance values due to a larger change in the oxidation state. In combination with a wider potential window in comparison to the acidic electrolytes, the pseudocapacitive charge storage in neutral aqueous WIS electrolytes may lead to the development of energy storage devices with competitive energy density, enhanced safety, excellent power, and prolonged lifetimes.

This work shows that pseudocapacitive Li^+ intercalation can be considerably intensified by partial electrochemical oxidation of $Ti_3C_2T_x$ in neutral WIS electrolytes. The surface redox process increases the capacitance of $Ti_3C_2T_x$ by ~54% in the same electrolyte. An *in situ* XANES analysis reveals that Li^+ intercalation is accompanied by a surface redox reaction involving the oxidation state change of Ti atoms. The reversible oxidation/reduction of Ti atoms during Li^+ intercalation/deintercalation was further confirmed by an *in situ* EXAFS analysis, which recorded the expansion/contraction of the local bond length during electrochemical cycling of the partially oxidized $Ti_3C_2T_x$. The partially oxidized $Ti_3C_2T_x$ shows a slightly higher Ti valence in comparison to the pristine material, explaining the enhanced Ti reduction at a less negative potential. This work shows the possibility of tuning the initial valence of the transition metal in MXenes to increase the surface redox contribution, which may benefit the design of other MXene-based energy storage devices for operation in various types of electrolytes.[12,27]

■ ASSOCIATED CONTENT

Supporting Information

The Supporting Information is available free of charge at https://pubs.acs.org/doi/10.1021/acsenergylett.1c02262.

Supplementary figures as described in the text and experimental details, materials, and methods (PDF)

■ AUTHOR INFORMATION

Corresponding Author

Yury Gogotsi − *A. J. Drexel Nanomaterials Institute, and Department of Materials Science and Engineering, Drexel University, Philadelphia, Pennsylvania 19104, United States;* orcid.org/0000-0001-9423-4032; Email: gogotsi@drexel.edu

Authors

Xuehang Wang − *A. J. Drexel Nanomaterials Institute, and Department of Materials Science and Engineering, Drexel University, Philadelphia, Pennsylvania 19104, United States; Storage of Electrochemical Energy (SEE), Department of Radiation Science and Technology, Delft University of Technology, Delft 2629 JB, The Netherlands;* orcid.org/0000-0002-8984-6162

Seong-Min Bak − *National Synchrotron Light Source II, Brookhaven National Laboratory, Upton, New York 11973, United States;* orcid.org/0000-0002-1626-5949

Meikang Han − *A. J. Drexel Nanomaterials Institute, and Department of Materials Science and Engineering, Drexel University, Philadelphia, Pennsylvania 19104, United States;* orcid.org/0000-0003-3309-988X

Christopher E. Shuck − *A. J. Drexel Nanomaterials Institute, and Department of Materials Science and Engineering, Drexel University, Philadelphia, Pennsylvania 19104, United States;* orcid.org/0000-0002-1274-8484

Conlan McHugh − *A. J. Drexel Nanomaterials Institute, and Department of Materials Science and Engineering, Drexel University, Philadelphia, Pennsylvania 19104, United States*

Ke Li − *A. J. Drexel Nanomaterials Institute, and Department of Materials Science and Engineering, Drexel University, Philadelphia, Pennsylvania 19104, United States;* orcid.org/0000-0002-1402-4893

Jianmin Li − *A. J. Drexel Nanomaterials Institute, and Department of Materials Science and Engineering, Drexel University, Philadelphia, Pennsylvania 19104, United States;* orcid.org/0000-0002-1162-9301

Jun Tang − *A. J. Drexel Nanomaterials Institute, and Department of Materials Science and Engineering, Drexel University, Philadelphia, Pennsylvania 19104, United States*

Complete contact information is available at: https://pubs.acs.org/10.1021/acsenergylett.1c02262

Author Contributions

[‖]X.W. and S.-M.B. contributed equally to this work.

Notes

The authors declare no competing financial interest.

■ ACKNOWLEDGMENTS

This research was sponsored by the Fluid Interface Reactions, Structures and Transport (FIRST) Center, an Energy Frontier Research Center funded by the US Department of Energy, Office of Science, and Office of Basic Energy Sciences. The XAS research used beamline 7-BM (QAS) and 21-ID-2 (EMS) of the National Synchrotron Light Source II, a US Department of Energy (DOE) Office of Science User Facility operated for the DOE Office of Science by Brookhaven National Laboratory under Contract No. DE-SC0012704. This research used resources of the Center for Functional Nanomaterials, which is a US DOE Office of Science Facility, at Brookhaven National Laboratory under Contract No. DE-SC0012704. The authors would also like to acknowledge the usage of the X-ray diffractometers provided by Drexel University Materials Characterization Core (MCC). X.W.'s research at Drexel University was supported by a Cotswold Foundation Postdoctoral Fellowship.

REFERENCES

(1) Simon, P.; Gogotsi, Y. Perspectives for Electrochemical Capacitors and Related Devices. *Nat. Mater.* **2020**, *19* (11), 1151−1163.

(2) Fleischmann, S.; Mitchell, J. B.; Wang, R.; Zhan, C.; Jiang, D.-e.; Presser, V.; Augustyn, V. Pseudocapacitance: From Fundamental Understanding to High Power Energy Storage Materials. *Chem. Rev.* **2020**, *120* (14), 6738−6782.

(3) Anasori, B.; Lukatskaya, M. R.; Gogotsi, Y. 2D Metal Carbides and Nitrides (MXenes) for Energy Storage. *Nat. Rev. Mater.* **2017**, *2*, 16098.

(4) Naguib, M.; Kurtoglu, M.; Presser, V.; Lu, J.; Niu, J.; Heon, M.; Hultman, L.; Gogotsi, Y.; Barsoum, M. W. Two-Dimensional Nanocrystals Produced by Exfoliation of Ti_3AlC_2. *Adv. Mater.* **2011**, *23* (37), 4248−4253.

(5) Deysher, G.; Shuck, C. E.; Hantanasirisakul, K.; Frey, N. C.; Foucher, A. C.; Maleski, K.; Sarycheva, A.; Shenoy, V. B.; Stach, E. A.; Anasori, B.; et al. Synthesis of Mo_4VAlC_4 MAX Phase and Two-Dimensional Mo_4VC_4 MXene with Five Atomic Layers of Transition Metals. *ACS Nano* **2020**, *14* (1), 204−217.

(6) Lukatskaya, M. R.; Kota, S.; Lin, Z.; Zhao, M.-Q.; Shpigel, N.; Levi, M. D.; Halim, J.; Taberna, P.-L.; Barsoum, M. W.; Simon, P.; Gogotsi, Y. Ultra-High-Rate Pseudocapacitive Energy Storage in Two-Dimensional Transition Metal Carbides. *Nat. Energy* **2017**, *2*, 17105.

(7) Lukatskaya, M. R.; Bak, S. M.; Yu, X.; Yang, X. Q.; Barsoum, M. W.; Gogotsi, Y. Probing the Mechanism of High Capacitance in 2D Titanium Carbide Using in Situ X-Ray Absorption Spectroscopy. *Adv. Energy Mater.* **2015**, *5* (15), 1500589.

(8) Yang, Y.; Hantanasirisakul, K.; Frey, N. C.; Anasori, B.; Green, R. J.; Rogge, P. C.; Waluyo, I.; Hunt, A.; Shafer, P.; Arenholz, E.; et al. Distinguishing Electronic Contributions of Surface and Sub-Surface Transition Metal Atoms in Ti-Based MXenes. *2D Mater.* **2020**, *7* (2), 025015.

(9) Lukatskaya, M. R.; Mashtalir, O.; Ren, C. E.; Dall'Agnese, Y.; Rozier, P.; Taberna, P. L.; Naguib, M.; Simon, P.; Barsoum, M. W.; Gogotsi, Y. Cation Intercalation and High Volumetric Capacitance of Two-Dimensional Titanium Carbide. *Science* **2013**, *341* (6153), 1502−1505.

(10) Sugahara, A.; Ando, Y.; Kajiyama, S.; Yazawa, K.; Gotoh, K.; Otani, M.; Okubo, M.; Yamada, A. Negative Dielectric Constant of Water Confined in Nanosheets. *Nat. Commun.* **2019**, *10* (1), 850.

(11) Okubo, M.; Sugahara, A.; Kajiyama, S.; Yamada, A. MXene as a Charge Storage Host. *Acc. Chem. Res.* **2018**, *51* (3), 591−599.

(12) Wang, X.; Mathis, T. S.; Li, K.; Lin, Z.; Vlcek, L.; Torita, T.; Osti, N. C.; Hatter, C.; Urbankowski, P.; Sarycheva, A.; et al. Influences from Solvents on Charge Storage in Titanium Carbide MXenes. *Nat. Energy* **2019**, *4* (3), 241−248.

(13) Li, Y.; Shao, H.; Lin, Z.; Lu, J.; Liu, L.; Duployer, B.; Persson, P. O.; Eklund, P.; Hultman, L.; Li, M.; et al. A General Lewis Acidic Etching Route for Preparing MXenes with Enhanced Electrochemical Performance in Non-Aqueous Electrolyte. *Nat. Mater.* **2020**, *19* (8), 894−899.

(14) Kim, K.; Ando, Y.; Sugahara, A.; Ko, S.; Yamada, Y.; Otani, M.; Okubo, M.; Yamada, A. Dense Charge Accumulation in MXene with a Hydrate-Melt Electrolyte. *Chem. Mater.* **2019**, *31* (14), 5190−5196.

(15) Kim, K.; Okubo, M.; Yamada, A. Interfacial Dissociation of Contact-Ion-Pair on MXene Electrodes in Concentrated Aqueous Electrolytes. *J. Electrochem. Soc.* **2019**, *166* (15), A3739.

(16) Avireddy, H.; Byles, B. W.; Pinto, D.; Galindo, J. M. D.; Biendicho, J. J.; Wang, X.; Flox, C.; Crosnier, O.; Brousse, T.; Pomerantseva, E.; et al. Stable High-Voltage Aqueous Pseudocapacitive Energy Storage Device with Slow Self-Discharge. *Nano Energy* **2019**, *64*, 103961.

(17) Wang, X.; Mathis, T. S.; Sun, Y.; Tsai, W.-Y.; Shpigel, N.; Shao, H.; Zhang, D.; Hantanasirisakul, K.; Malchik, F.; Balke, N.; et al. Titanium Carbide MXene Shows an Electrochemical Anomaly in Water-in-Salt Electrolytes. *ACS Nano* **2021**, *15* (9), 15274−15284.

(18) Suo, L.; Borodin, O.; Gao, T.; Olguin, M.; Ho, J.; Fan, X.; Luo, C.; Wang, C.; Xu, K. "Water-in-Salt" Electrolyte Enables High-Voltage Aqueous Lithium-Ion Chemistries. *Science* **2015**, *350* (6263), 938−943.

(19) Tang, J.; Mathis, T. S.; Kurra, N.; Sarycheva, A.; Xiao, X.; Hedhili, M. N.; Jiang, Q.; Alshareef, H. N.; Xu, B.; Pan, F.; et al. Tuning the Electrochemical Performance of Titanium Carbide MXene by Controllable *in Situ* Anodic Oxidation. *Angew. Chem., Int. Ed.* **2019**, *58* (49), 17849−17855.

(20) Cao, M.; Wang, F.; Wang, L.; Wu, W.; Lv, W.; Zhu, J. Room Temperature Oxidation of Ti_3C_2 MXene for Supercapacitor Electrodes. *J. Electrochem. Soc.* **2017**, *164* (14), A3933.

(21) Mathis, T. S.; Kurra, N.; Wang, X.; Pinto, D.; Simon, P.; Gogotsi, Y. Energy Storage Data Reporting in Perspective—Guidelines for Interpreting the Performance of Electrochemical Energy Storage Systems. *Adv. Energy Mater.* **2019**, *9* (39), 1902007.

(22) Forghani, M.; Donne, S. W. Method Comparison for Deconvoluting Capacitive and Pseudo-Capacitive Contributions to Electrochemical Capacitor Electrode Behavior. *J. Electrochem. Soc.* **2018**, *165* (3), A664.

(23) Bak, S. M.; Qiao, R.; Yang, W.; Lee, S.; Yu, X.; Anasori, B.; Lee, H.; Gogotsi, Y.; Yang, X. Q. Na-Ion Intercalation and Charge Storage Mechanism in 2D Vanadium Carbide. *Adv. Energy Mater.* **2017**, *7* (20), 1700959.

(24) Nam, K.-W.; Kim, M. G.; Kim, K.-B. In Situ Mn K-Edge X-Ray Absorption Spectroscopy Studies of Electrodeposited Manganese Oxide Films for Electrochemical Capacitors. *J. Phys. Chem. C* **2007**, *111* (2), 749−758.

(25) Krayzman, V.; Levin, I.; Woicik, J.; Yoder, D.; Fischer, D. Effects of Local Atomic Order on the Pre-Edge Structure in the Ti K X-Ray Absorption Spectra of Perovskite $CaTi_{1-x}Zr_xO_3$. *Phys. Rev. B: Condens. Matter Mater. Phys.* **2006**, *74* (22), 224104.

(26) Handoko, A. D.; Fredrickson, K. D.; Anasori, B.; Convey, K. W.; Johnson, L. R.; Gogotsi, Y.; Vojvodic, A.; Seh, Z. W. Tuning the Basal Plane Functionalization of Two-Dimensional Metal Carbides (MXenes) to Control Hydrogen Evolution Activity. *ACS Appl. Energy Mater.* **2018**, *1* (1), 173−180.

(27) Li, X.; Ma, X.; Hou, Y.; Zhang, Z.; Lu, Y.; Huang, Z.; Liang, G.; Li, M.; Yang, Q.; Ma, J.; et al. Intrinsic Voltage Plateau of a Nb_2CT_x MXene Cathode in an Aqueous Electrolyte Induced by High-Voltage Scanning. *Joule* **2021**, *5*, 2993.

https://doi.org/10.1021/acsenergylett.1c02262
ACS Energy Lett. 2022, 7, 30−35